Evaluation of domain models for β-cristobalite from the pair distribution function

2010 J. Phys.: Condens. Matter 22 125401

(http://iopscience.iop.org/0953-8984/22/12/125401)

J. Phys.: Condens. Matter **22** (2010) 125401 (7pp) doi:10.1088/0953-8984/22/12/125401

Evaluation of domain models for β-cristobalite from the pair distribution function

Elizabeth R Cope and Martin T Dove

Department of Earth Sciences, University of Cambridge, Downing Street, Cambridge CB2 3EQ, UK

E-mail: ers29@cam.ac.uk and mtd10@cam.ac.uk

Received 17 December 2009
Published 8 March 2010
Online at stacks.iop.org/JPhysCM/22/125401

Abstract

We address the question of whether the structural disorder in the high-temperature β-cristobalite phase of silica can be explained on the basis of domain models using a new technique of phonon-based computer simulations of the pair distribution function. None of the domain models give as good an agreement to experimental data as previously reported atomic configurations derived from a reverse Monte Carlo analysis that are consistent with the rigid unit mode model.

(Some figures in this article are in colour only in the electronic version)

1. Introduction

The atomic structure of the high-temperature β-phase of cristobalite, SiO_2, has long elicited a controversy that remains unresolved. Whilst the average structure is undisputed—cubic $Fd\bar{3}m$ space group, Si atoms occupying sites that form a diamond lattice, and O atoms having average positions mid-way between Si atoms [1–3]—and whilst it is also generally accepted that the structure must be disordered, there is no consensus as to the nature of the disorder.

The main reason for believing that the structure of β-cristobalite is disordered is that a literal interpretation of the structure described above would mean the Si–O bond has length 1.55 Å and an Si–O–Si bond angle of 180°, in contrast to typical values for silica and silicate structures of ∼1.61 Å and ∼145° respectively, as in the structure of low-temperature α-cristobalite [3, 4]. Crystal structure refinements of β-cristobalite based on this idealized structure show a wide distribution of displacements of the oxygen atoms in directions normal to the Si–Si vector, which suggests either large thermal fluctuations or, more likely, some degree of disorder in the actual positions of the oxygen atoms [1, 3, 5, 6].

The rigidity of SiO_4 tetrahedra means that large-amplitude rotations of the Si–O bond can only occur by rotating the tetrahedra, and since neighbouring tetrahedra are linked into an infinite network a rotation of one tetrahedron will necessitate coupled rotations of surrounding tetrahedra. Thus the question that is often posed, even if only implicitly, is how to create disorder on a local scale whilst preserving the integrity of the tetrahedra? The importance of this question transcends the specific example of cristobalite; this issue is encountered, for example, in attempts to understand the relationship between structural fluctuations and physical properties, such as negative thermal expansion [7].

Within the literature there are two approaches for understanding this disorder, based either on the existence of domains or on rigid unit modes (RUMs). However, to date there has been no attempt to assess the relative merits of the domain models, and no means to compare them to the RUM model at the appropriate length scale. The key experimental probe required to assess the validity of the various models on an experimental basis is measurement of the pair distribution function (PDF) [3] which can reveal fluctuations of the local structure that give rise to significant differences from the average structure.

Data for the PDF of the two phases of cristobalite were first reported in 1997 [5] and subsequently analysed using the reverse Monte Carlo (RMC) method [6]. The important information provided by the experimental PDF was that the average instantaneous Si–O bond lengths are indeed around 1.61 Å over a wide range of temperature, and the PDF data for O–O and Si–Si distance can be best understood with an average Si–O–Si angle of 146° and ideal tetrahedral geometry of the SiO_4 units [5]. This immediately confirmed that the local

structure of β-cristobalite must arise through rotations of the SiO_4 tetrahedra.

The recent development of a simulation tool for the full calculation of the PDF for any structural model [8], where peak widths are computed from a lattice dynamics calculation, finally allows a quantitative analysis of the various models for the disorder in β-cristobalite though comparison with experimental data. Thus the primary aim of this work is to use this new approach to resolve the controversy surrounding the local structure of β-cristobalite. We begin with a historical review of the various models, followed by a brief description of our approach. Finally, we discuss the detailed comparison of predictions from different models and experimental data.

2. Historical survey of models of disorder in β-cristobalite

2.1. Multi-site models

The first attempt to describe a disordered atomic structure of β-cristobalite was to assume that the O atoms occupy six positions in a ring around the mean position, each with a fractional mean occupancy of 1/6 [1, 9]. This allows better agreement between the calculated and observed diffraction patterns than using the ideal cubic structure, giving bond lengths and angles that match the PDF analysis [1, 3, 5, 6]. However, the model does not address the issue of how the disorder can be accommodated when it requires rotations of whole SiO_4 tetrahedra. Moreover, it is not easy to differentiate between a multi-site model and a continuous distribution of atomic positions because the distance between neighbouring oxygen sites in this model is comparable with the resolution of the diffraction experiment[1]. The problem is amplified when thermal motion is included—see figure 1 in [6] which shows how thermal fluctuations smear the distribution of O atoms when described using the six-site model.

2.2. Domain models

The most popular interpretation of the structural disorder has been to assume that the local structure consists of domains of a lower-symmetry phase, with the average cubic symmetry arising as an average over all possible orientations of these domains. The first domain model was proposed by Wright and Leadbetter (WL) [2], and this was followed by an alternative model proposed by Hatch and Ghose (HG) [10]. A search of the Science Citation Index at the time of submission highlights the fact that the WL model has gained more popularity than the HG model in the literature and is frequently being used in simulation papers as the starting point for static energy calculations (such as Jiang *et al* [11] and Arasa *et al* [12]), although neither model has been subjected to detailed scrutiny.

[1] The maximum scattering vector Q obtainable with conventional diffraction, $Q_{max} = 2\pi/d_{min}$, leads to the best resolution in any refined real-space structure of $\Delta r = 2\pi/Q_{max} = d_{min}$, where d_{min} is the minimum d-spacing observed in the diffraction pattern. For x-ray diffraction experiments using standard Cu Kα radiation, the best real-space resolution possible is $\Delta r \sim 0.8$ Å. Using neutron diffraction from spallation source as in [3] can further improve this. Total scattering experiments extend the Q range so the resolution is even finer: the data used in this paper have a resolution of 0.13 Å.

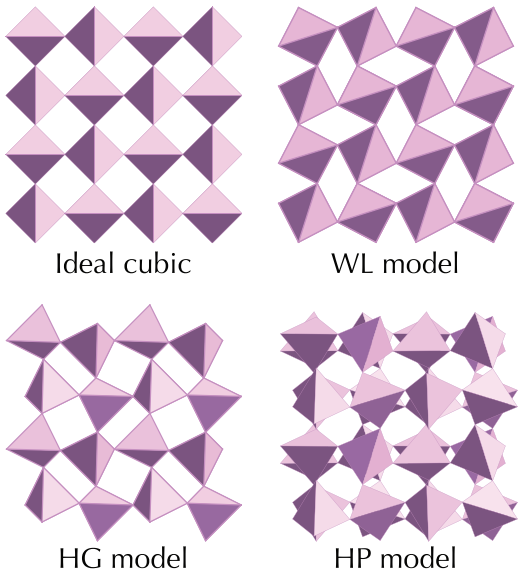

Figure 1. Comparison of the ideal cubic representation of the crystal structure of β-cristobalite with the crystal structures of the WL model (space group $I\bar{4}2d$, viewed down the tetragonal [0, 0, 1] axis), the HG model (experimental α-phase, space group $P4_12_12$, viewed down the tetragonal [0, 0, 1] axis), and the HP phase (experimental high-pressure phase, space group $P2_1/c$, viewed down the [2, 0, 1] direction). These structures correspond to modulations having wavevectors located at different points on the surface of the Brillouin zone of the ideal cubic structure. SiO_4 tetrahedra are highlighted as shaded solid objects. Model structures were obtained using lattice energy minimization as described in the text.

2.2.1. The WL model. The WL model [2] proposes that the disorder is accommodated by a local distortion of the crystal structure into a tetragonal form of space group $I\bar{4}2d$. Here, the cubic phase results from disorder over all possible orientations of small domains of this structure. In fact, WL suggested that a domain could be as small as one unit cell. The structure proposed by WL is shown in figure 1: it is derived from the ideal cubic structure (also shown) by a rotation of the tetrahedra about the [0, 0, 1] axis. This distortion corresponds to a phonon mode of zero wavevector (the Γ point at the centre of the Brillouin zone). The lattice parameters for this model (after lattice energy minimization, see section 3.3) are $a = 5.028$ Å and $c = 7.205$ Å, with a mean Si–O distance of 1.597 Å.

2.2.2. The HG model. In the HG model [10] the disorder arises from all 12 orientations of domains of the tetragonal low-temperature α form of cristobalite. The structure can be compared with the ideal cubic and WL structures in figure 1. Here, tetrahedra are rotated about axes parallel to the horizontal and vertical directions in the plane of the diagram (orthogonal axes normal to the [0, 0, 1] axis). This distortion arises from a phonon mode with wavevector $\mathbf{k} = (1, 0, 0)$, corresponding to the X-point on the face of the Brillouin zone. The lattice parameters for this model (after lattice energy minimization) are $a = 5.010$ Å and $c = 7.062$ Å, with a mean Si–O distance of 1.597 Å.

2.3. The rigid unit mode model and evidence from reverse Monte Carlo simulations

Analysis of the rigidity of a model structure based on fixed SiO_4 tetrahedra with flexible linkages at the shared corners showed the existence of planes of wavevectors in which one or more phonons could propagate without deforming the tetrahedra [13, 14]. These phonons, called rigid unit modes (RUMs), will have low frequency because they do not involve the larger force constants associated with deformations of the tetrahedra. The prediction of planes of low-frequency modes in β-cristobalite exactly matches the diffuse scattering seen in transmission electron diffraction [15]. Thus our group in Cambridge proposed that the disorder in the cubic β-cristobalite arises from the dynamic superposition of all RUMs across the planes of wavevectors, giving large contributions to the atomic motions because their amplitudes scale as $1/\omega^2$. This interpretation has been supported by a number of independent simulation studies [16] as well as our own model simulations [17]. The RUM model predicts the existence of the soft mode for the β–α transition as seen in spectroscopic measurements in an α-phase [18, 19], as well as giving low-frequency phonons that can provide transition pathways between the different phases.

Reverse Monte Carlo (RMC) [20] simulations based on experimental total scattering data [6] showed a number of features supporting the RUM model. These include reproducing three-dimensional diffuse scattering patterns predicted by the RUM model and as seen in electron diffraction, and that the oxygen atoms are continuously distributed on a broad annulus around the Si–Si vector rather than occupying specific sites. Analysis of the configurations showed that the most significant contributions to atomic motions arose from SiO_4 tetrahedra moving as rigid bodies [21].

2.4. A new domain model: the HP model

Given that the popular domain models are formed by deformation of the ideal cubic structure by the eigenvectors of specific RUMs, we note that it would be equally credible to construct a domain model based instead on the structure of the high-pressure monoclinic phase [22]. This structure is derived from the parent cubic structure by a more complex set of rotations involving unequal rotations of the SiO_4 tetrahedra about two orthogonal axes with wavevector $\mathbf{k} = (\frac{1}{2}, \frac{1}{2}, \frac{1}{2})$, corresponding to the L-point on the face of the Brillouin zone. This is compared with the other structures in figure 1. The lattice parameters for this model (after lattice energy minimization) are $a = 8.739$ Å, $b = 5.017$ Å, $c = 10.067$ Å and $\beta = 125.2°$, with a mean Si–O distance of 1.597 Å.

2.5. Is there a way to reconcile the models?

The three domains discussed above all represent distortions of the cubic structure via condensation of individual RUMs of β-cristobalite. Thus the RUM model of disorder will include fluctuations into each of the domain model phases considered here, but will also include a myriad of other fluctuations with a range of wavevectors. Whilst all three domain structures are symmetry subgroups of the parent cubic symmetry, they are not subgroups of each other but instead are orthogonal deformations of the structure. There is no *a priori* reason to suggest a preference of either the WL, HG or HP structures over the others as candidates for any domain model, but it is possible that one domain fluctuation might be particularly important. This has not yet been tested.

All models imply a length scale over which the local symmetry will be lower than the average symmetry, which might enable certain anomalies in the spectroscopy to be understood[2]. This being so, the critical issue is to understand the structure in terms of its short-range order and fluctuations. We now discuss the approach of using the PDF—which uniquely probes the relevant length scales—to compare the predictions of the domain models against experimental data.

3. The pair distribution function

3.1. Formalism

The PDF is derived experimentally by Fourier transform of the observed total scattering function from neutron or x-ray diffraction experiments [24]. It can also be calculated from phonon modes using the theory of Chung and Thorpe [25]. The crystal structure gives peak positions and integrated areas, while the phonons give the temperature-dependent widths.

Following Keen [24], the scattering function $S(Q)$ can be written as

$$S(Q) = \frac{1}{N}\sum_{j,k} b_j b_k \frac{\sin(Q|\mathbf{r}_j - \mathbf{r}_k|)}{Q\,|\mathbf{r}_j - \mathbf{r}_k|} \tag{1}$$

$$= i(Q) + \sum_m c_m \langle b_m^2 \rangle, \tag{2}$$

where Q is the modulus of the scattering vector, N is the number of atoms, j and k label different atoms, b_j is the scattering length of atom j, $\mathbf{r}_j$ is the instantaneous position of atom j, m represents an atom type, and c_m is the number concentration of atom type m. The function $i(Q)$ is related to the PDF, $D(r)$, by

$$Qi(Q) = \rho_0 \int D(r)\sin(Qr)\,\mathrm{d}r, \tag{3}$$

where ρ_0 is the number of atoms per unit volume. $D(r)$ is the form of the PDF particularly convenient for studying mid-range structural detail, and related to the $g(r)$ and weighted

[2] In both the infrared and Raman spectra there is one mode in the α phase that remains on heating above the α–β phase transition but that should be absent by symmetry in the β phase; in contrast, all other vibrations expected to disappear at the phase transition do in fact do so [18]. Thus Zhang *et al* [19] proposed that we should go back to the WL model as the best approach to understanding the structure of β-cristobalite. They also suggested that the structure of the α phase, about which there has been no controversy, should also be assigned to a lower-symmetry structure. Coh and Vandebilt [23] carried out an analysis of the phonons in the WL structure based on *ab initio* DFT methods, showing that the anomalous IR mode can be understood on the basis of the existence of domains of the WL structure.

$d'(r)$ partial PDFs through

$$D(r) = 4\pi r\rho_0 \sum_{m,n} c_m c_n \bar{b}_m \bar{b}_n (g_{m,n}(r) - 1) \quad (4)$$

$$= \sum_{m,n} d'_{m,n}(r) \quad (5)$$

with $\bar{b}_m$ as the coherent scattering length of atom type m.

For harmonic phonons, the peaks in $g(r)$ have Gaussian shapes with area proportional to the number of neighbours, and temperature-dependent widths that are obtained by summing over all phonons. The formalism described by Chung and Thorpe [25] for the computation of a PDF has been implemented for interatomic potential models by ourselves [8].

3.2. Experimental data

We use the published neutron scattering measurements of the PDF of cristobalite [5, 6] for comparison with the calculations presented in this paper. The data were collected on the LAD diffractometer [26] at the ISIS spallation neutron source; details are given in the primary references [5, 6]. The large Q-range on LAD yields excellent resolution in the real-space PDF, and for a crystal of cubic symmetry and modest size unit cell it has adequate Q-space resolution. A Monte Carlo approach was used to obtain the PDF from the total scattering data—this method enforces the absence of Fourier ripples before the first peak [27]. Experimental data are available for both phases of cristobalite, collected at temperatures of 475 K (α) and 575, 700 and 825 K (β). The measured PDFs of the two phases show significant differences for distances beyond the nearest-neighbour Si–O, O–O and Si–Si peaks, as noted in the original publication [5]. On the other hand, there appears to be little difference in the measured PDFs of the β phase at different temperatures.

Published RMC analysis [6] of total scattering is used for comparison with the domain models. The RMC method [20] enables the total PDF to be interpreted in terms of partial PDFs, $d'_{m,n}(r)$. These are shown in figure 2 to facilitate interpretation of the individual peaks in the PDF. It is clear that beyond the first two peaks the various features in the experimental PDF correspond to contributions from more than one atom pair.

3.3. Simulation

Computer simulations were performed using the GULP lattice simulation program [28], with our new PDF module [8]. We use the popular and highly transferable empirical potential model of Sanders *et al* [29], which we have shown gives a good PDF for α-cristobalite [8] and α-quartz (unpublished). Each structure was relaxed to give the minimum lattice energy, and phonon calculations were performed using these relaxed structures.

Convergence of the PDF peak widths was obtained using a standard Monkhorst–Pack grid [30] with 35 points along each reciprocal lattice vector and 42 875 wavevectors within the first Brillouin zone. PDFs were computed for the same temperatures as in the experiments.

From our previous work [8] we expect the Sanders [29] model to reproduce the positions of the main features in $D(r)$ to within 2–3%. Larger differences would mean that the calculation and experiment are not in agreement. In this regard we note that the main features in the experimental PDFs of both phases of cristobalite show considerable differences beyond the first Si–Si peak (peak three).

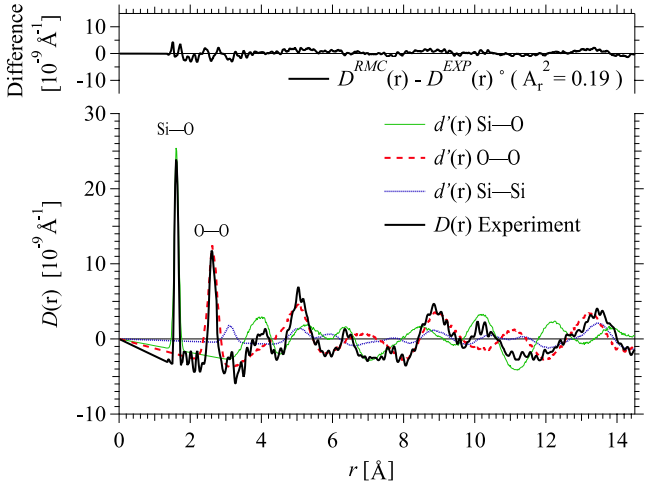

Figure 2. $D(r)$ of β-cristobalite (SiO_2) at 700 K showing how the (weighted) partial pair distributions for each atom type make up the total $D(r)$ (experimental data shown with a thick black line). The difference plot shows the excellent agreement between the RMC model (the sum of the partials shown) and the experimental data, giving an A_r^2 agreement factor of 0.19 (defined below).

3.4. Agreement factors

To compare the relative agreements between calculated and experimental PDFs for different structural models we give plots of the differences. We also define a quantitative agreement factor. Since $D(r)$ oscillates around zero at high r, it is not appropriate for use in a 'sum-of-residuals' type agreement factor, so the data were converted[3] to density functions $\rho^{\mathrm{PDF}}(r)$ [24, 31] via

$$\rho^{\mathrm{PDF}}(r) = \rho_0 + \frac{D(r)}{4\pi r(\sum_m c_m \bar{b}_m)^2}. \quad (6)$$

This is the form of the pair distribution function used in the standard agreement factor of Toby and Egami [31] (which mirrors the R-factor used in crystal structure refinement). However, the data presented here is in the r-weighted $D(r)$ format (which is particularly suited to examining mid-range structural detail). Therefore, we define a new agreement factor to take appropriate account of the higher-r features.

$$A_r^2 = \frac{1}{n\rho_0^2} \sum_{l=1}^{n} \left[r\rho_{\mathrm{obs}}^{\mathrm{PDF}}(r_l) - r\rho_{\mathrm{model}}^{\mathrm{PDF}}(r_l) \right]^2 \Delta r, \quad (7)$$

where Δr is the spacing of n points. Agreement factors are calculated across the entire range of the graphs presented.

To aid interpretation of the agreement factors, we note that comparing the experimental PDF data for α and β phases gives a value of $A_r^2 = 0.66$.

[3] As the different structures optimized to slightly different unit cells, the number density also varied slightly. For consistency, the same number density (0.067 Å^{-3}) was used for all calculations of agreement factors.

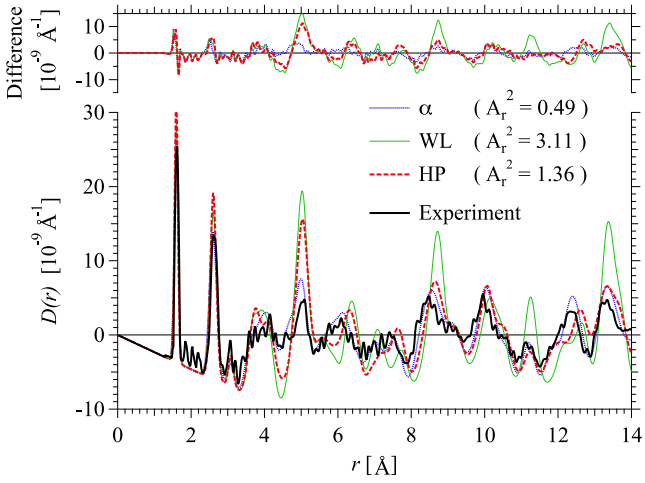

Figure 3. $D(r)$ of α-cristobalite (SiO_2) at 475 K comparing experimental data (thick black line) with the three structural models discussed in the text. This shows how well the simulation can reproduce experimental data for a known structural model. Dotted blue line: actual α-cristobalite structure. Solid green line: WL $I\bar{4}2d$ structure. Dashed red line: HP $P2_1/c$ structure. The difference plot is shown above the main figure, using the same colours.

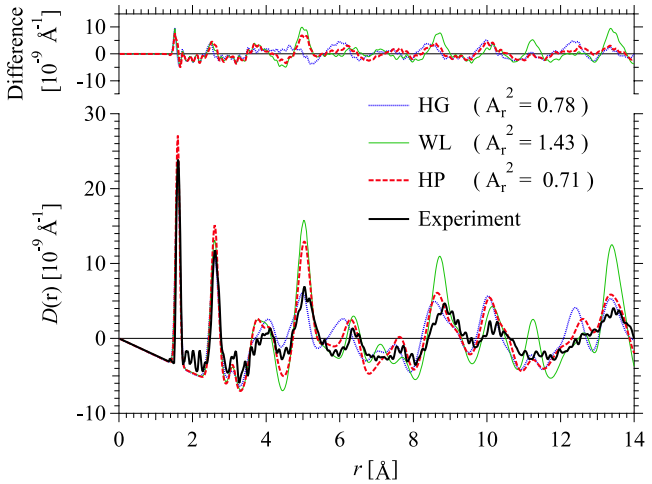

Figure 4. $D(r)$ of β-cristobalite (SiO_2) at 700 K comparing experimental data (thick black line) with the three structural models discussed in the text. Dotted blue line: HG model (domains of α-cristobalite structure). Solid green line: WL model (domains of $I\bar{4}2d$ structure). Dashed red line: HP model (domains of high-pressure $P2_1/c$ structure). The difference plot is shown above the main figure, using the same colours.

4. Results, discussion and conclusions

4.1. A benchmark from analysis of α-cristobalite

Benchmarks for both good and poor agreement are provided by comparing computed PDFs of each model with α-cristobalite experimental data, figure 3. The HG model is expected to give good agreement in this case, as this model is that of α-cristobalite. On the other hand, the WL and HP models should give poor agreement. Thus $A_r^2 = 0.49$ obtained for the HG model contrasts with $A_r^2 = 3.11$ and $A_r^2 = 1.38$ for the WL and HP structures. Figure 3 shows how the difference plot and peak positions, widths and intensities reflect the level of agreement with experimental data.

4.2. Evaluation of domain models for β-cristobalite

The β-cristobalite experimental data and the three proposed domain models are compared in figure 4. A close match for nearest-neighbour Si–O, O–O and Si–Si peaks is seen in all structures, reflecting the fact that all models have nearly perfect SiO_4 tetrahedra. There is reasonable agreement with the positions of the two features at around 4 and 5 Å in the overall PDF—from figure 2 we note that these correspond to peaks in both the Si–O and O–O partial PDFs—but although the positions of these features match the data, the widths given by the WL and HP models are significantly different from experiment.

The WL model matches the positions of several features in the experimental PDF up to about 10 Å, and beyond the first five peaks gives a better fit to the position of peaks than the HG model. However, features in the WL model are significantly sharper than for experiment. This enhanced sharpening arises from the fact that the WL model crystal structure is simpler than the other models, so the peak broadening arises mostly from phonon broadening rather than the overlap of several atom-pair peaks with similar r. The WL model shows a notable difference from the experimental PDF at around 11 Å. The agreement factor has a value of $A_r^2 = 1.43$, showing that the WL model no more corresponds to the β-cristobalite data than the HP model corresponds to the α-cristobalite phase. The WL model clearly gives a 'poor fit' according to our benchmarks.

There is significant disagreement between the HG and experimental PDF beyond the first five peaks, starting clearly with the first feature at 6.4 Å. Subsequent features become out of register; for example, features at distances between 8 and 11 Å are at slightly lower r, and the predicted peak at 12.5 Å is not reflected in the experimental data. These discrepancies are consistent with differences between experimental PDFs for the two phases of cristobalite noted previously [5], and their effects are seen in the larger agreement factor of $A_r^2 = 0.78$ in the β-phase.

Finally, the HP domain model yields a similar level of agreement in its PDF to the HG domain model. It shows a reasonably good register of corresponding features between data and simulation, although the peak at 5 Å is too narrow. Like the WL model, the HP model gives a better fit than the HG model in the region of 6.4 and 12.2 Å due to having a more complex structure. This is reflected in the agreement factor, $A_r^2 = 0.71$, which is comparable to that obtained with the HG structures. Again, this falls outside our benchmark for a good agreement.

4.3. Discussion and conclusions

The purpose of this paper has been to assess how far these popular models stand up to analysis with the recently developed phonon-based simulation tools. It is immediately obvious that none of the domain models have sufficient flexibility to accurately reproduce the experimental PDF. They

all fail to give agreement factors in any way comparable to that of the α-cristobalite model to the α-cristobalite experimental data. However it is interesting to note that the HP domain model, which has not previously been considered as a possible domain structure, shows slightly closer agreement with experimental data than the WL and HG models at short length scales, while still breaking down on mid-range length scales (around 12.5 Å). We would therefore argue that no one domain model can explain the disorder in β-cristobalite. Having noted that the WL model in particular is widely used as the starting point for simulations, this result has far-reaching implications.

It is clear that the best description of the PDF comes from the models generated by the RMC approach [6], as is evident in the agreement factors. Given that the RMC method is driven by improving agreement to experimental data, this is not surprising. However, the degree to which this improves upon the domain models implies that the level of disorder in the RMC configuration realistically reproduces the experimental situation. While the agreement of the RMC results with data do not preclude other configurations with more constraints (e.g. a domain model) from giving similarly good agreement, our chief finding is that none of these models actually do so. Moreover, the RMC fits are consistent with the absence of domains, as demonstrated through the calculation of the bond orientational distribution function [6], and show a significant amount of RUM motion as seen in geometric algebra analysis [21].

Much of the discussion about the disorder and local structure of β-cristobalite concerns the length scale over which structural fluctuations depart from the average structure. This is where comparison of models against experimentally derived PDFs provides important quantitative information. Over length scales associated with Bragg diffraction, the space- and time-averaged structure has the ideal $Fd\bar{3}m$ structure, but over short length scales we expect fluctuations from this average structure. What we have shown in this paper is that the various domain models have PDFs that have some similarities to the experimental PDF, but beyond distances of around 10 Å the similarities are lost, and even at lower distances the experimental PDF of the WL model appears to underestimate the degree of structural disorder. We would argue that since this length scale does not extend much beyond the unit cell, a considerable volume (more than half) of any structure that consists of domains of one unit cell size will actually be domain walls, and these will be formed by RUM deformations for a wide range of wavevectors.

Furthermore, whilst the various domains discussed here will exist as fluctuations of the structure over a local length scale, we can preclude the possibility that the WL or HG domains will be dominant. By demonstrating that yet another RUM deformation can yield comparable or even closer agreement on the local scale, we find our results favouring the proposition [13, 14]—supported by the RMC analysis [6]—that the local fluctuations will correspond to Fourier superpositions of the planes of RUM phonons. The WL, HG and HP RUMs (Γ, X and L points respectively) will be included but will not be the only contributions. We anticipate that it will be possible to construct other types of domains from the known RUMs, which, like the HG, WL and HP models, preserve the size and shape of the SiO_4 tetrahedra. Extending the recent simulations on transition pathways between different domains [23] has the potential to add significantly to our understanding of the disorder in β-cristobalite.

Finally, in light of what our new approach has demonstrated, we strongly recommend that neither the WL nor HG domain models should be used as models for simulations involving β-cristobalite.

Acknowledgments

We thank Emilio Artacho (University of Cambridge) and Ian Swainson (NRC Chalk River) for helpful discussions. We acknowledge financial support from the Natural Environment Research Council (UK) and the Science and Technology Facilities Council.

References

[1] Peacor D R 1973 High-temperature single-crystal study of cristobalite inversion *Z. Kristallogr.* **138** 274–98
[2] Wright A F and Leadbetter A J 1975 Structures of β-cristobalite phases of SiO_2 and $AlPO_4$ *Phil. Mag.* **31** 1391–401
[3] Schmahl W W, Swainson I P, Dove M T and Graeme-Barber A 1992 Landau free energy and order parameter behaviour of the α/β phase transition in cristobalite *Z. Kristallogr.* **201** 125–45
[4] Pluth J J, Smith J V and Faber J 1985 Crystal structure of low cristobalite at 10, 293, and 473 K: variation of framework geometry with temperature *J. Appl. Phys.* **57** 1045–9
[5] Dove M T, Keen D A, Hannon A C and Swainson I P 1997 Direct measurement of the Si–O bond length and orientational disorder in the high-temperature phase of cristobalite *Phys. Chem. Miner.* **24** 311–7
[6] Tucker M G, Squires M P, Dove M T and Keen D A 2001 Dynamic structural disorder in cristobalite: neutron total scattering measurement and reverse Monte Carlo modelling *J. Phys.: Condens. Matter* **13** 403–23
[7] Barrera G D, Bruno J A O, Barron T H K and Allan N L 2005 Negative thermal expansionmal expansion *J. Phys.: Condens. Matter* **17** R217–52
[8] Cope E R and Dove M T 2007 Pair distribution functions calculated from interatomic potential models using the general utility lattice program *J. Appl. Crystallogr.* **40** 125–30
[9] Nieuwenkamp W 1937 On the structure of β cristobalite *Z. Kristallogr.* **96** 454–8
[10] Hatch D M and Ghose S 1991 The α–β phase transition in cristobalite, SiO_2 *Phys. Chem. Miner.* **17** 554–62
[11] Jiang D E and Carter E A 2005 First-principles study of the interfacial adhesion between SiO_2 and $MoSi_2$ *Phys. Rev.* B **72** 165410
[12] Arasa C, Busnengo H F, Salin A and Sayos R 2008 Classical dynamics study of atomic oxygen sticking on the β-cristobalite (100) surface *Surf. Sci.* **602** 975–85
[13] Swainson I P and Dove M T 1993 Low-frequency floppy modes in β-cristobalite *Phys. Rev. Lett.* **71** 193–6
[14] Hammonds K D, Dove M T, Giddy A P, Heine V and Winkler B 1996 Rigid-unit phonon modes and structural phase transitions in framework silicates *Am. Mineral.* **81** 1057–79

[15] Hua G L, Welberry T R, Withers R L and Thompson J G 1988 An electron-diffraction and lattice-dynamical study of the diffuse-scattering in β-cristobalite, SiO_2 *J. Appl. Crystallogr.* **21** 458–65
[16] Bourova E and Richet P 1998 Quartz and cristobalite: high-temperature cell parameters and volumes of fusion *Geophys. Res. Lett.* **25** 2333–6
[17] Gambhir M, Dove M T and Heine V 1999 Rigid unit modes and dynamic disorder: SiO_2 cristobalite and quartz *Phys. Chem. Miner.* **26** 484–95
[18] Swainson I P, Dove M T and Palmer D C 2003 Infrared and Raman spectroscopy studies of the α–β phase transition in cristobalite *Phys. Chem. Miner.* **30** 353–65
[19] Zhang M and Scott J F 2007 Raman studies of oxide minerals: a retrospective on cristobalite phases *J. Phys.: Condens. Matter* **19** 275201
[20] Tucker M G, Dove M T and Keen D A 2001 Application of the reverse Monte Carlo method to crystalline materials *J. Appl. Crystallogr.* **34** 630–8
[21] Wells S A, Dove M T, Tucker M G and Trachenko K 2002 Real-space rigid-unit-mode analysis of dynamic disorder in quartz, cristobalite and amorphous silica *J. Phys.: Condens. Matter* **14** 4645–57
[22] Dove M T, Craig M S, Keen D A, Marshall W G, Redfern S A T, Trachenko K O and Tucker M G 2000 Crystal structure of the high-pressure monoclinic phase-II of cristobalite, SiO_2 *Mineral. Mag.* **64** 569–76
[23] Coh S and Vanderbilt D 2008 Structural stability and lattice dynamics of SiO_2 cristobalite *Phys. Rev.* B **78** 054117
[24] Keen D A 2001 A comparison of various commonly used correlation functions for describing total scattering *J. Appl. Crystallogr.* **34** 172–7
[25] Chung J S and Thorpe M F 1999 Local atomic structure of semiconductor alloys using pair distribution functions. II *Phys. Rev.* B **59** 4807–12
[26] Howells W S and Hannon A C 1999 LAD, 1982–1998: the first ISIS diffractometer *J. Phys.: Condens. Matter* **11** 9127–38
[27] Tucker M G, Dove M T and Keen D A 2001 MCGRtof: Monte Carlo $G(r)$ with resolution corrections for time-of-flight neutron diffractometers *J. Appl. Crystallogr.* **34** 780–2
[28] Gale J D and Rohl A L 2003 The general utility lattice program (GULP) *Mol. Simul.* **29** 291–341
[29] Sanders M J, Leslie M and Catlow C R A 1984 Interatomic potentials for SiO_2 *J. Chem. Soc.-Chem. Commun.* **19** 1271–3
[30] Monkhorst H J and Pack J D 1976 Special points for Brillouin-zone integrations *Phys. Rev.* B **13** 5188–92
[31] Toby B H and Egami T 1992 Accuracy of pair distribution function-analysis applied to crystalline and non crystalline materials *Acta Crystallogr.* A **48** 336–46